

Determinants of Substrate and Cation Affinities in the Na⁺/Dicarboxylate Cotransporter[†]

Esther S. Kahn and Ana M. Pajor*

Department of Physiology, University of Arizona College of Medicine, Tucson, Arizona 85724

Received November 20, 1998; Revised Manuscript Received February 5, 1999

ABSTRACT: The Na⁺/dicarboxylate cotransporter (NaDC-1) couples the transport of sodium and tricarboxylic acid cycle intermediates, such as succinate and citrate. The rabbit and human homologues (rbNaDC-1 and hNaDC-1, respectively) are 78% identical in amino acid sequence but exhibit several differences in their functional properties. rbNaDC-1 has a greater apparent affinity for citrate and sodium than hNaDC-1. Furthermore, unlike hNaDC-1, rbNaDC-1 is inhibited by low concentrations of lithium. In this study, chimeric transporters were constructed to identify the protein domains responsible for the functional differences between rbNaDC-1 and hNaDC-1. Individual substitutions of transmembrane domain (TMD) 7, 10 or 11 produced transporters with intermediate properties. However, substitution of TMD 7, 10, and 11 together resulted in a transporter with the citrate *K_m* of the donor, suggesting that interactions between these domains determine the differences in apparent citrate affinities. TMDs 10 and 11 are most important in determining the differences in apparent sodium affinities, and TMD 11 determines the sensitivity to lithium inhibition. We conclude that transmembrane domains 7, 10, and 11 in NaDC-1 may contain at least one of the cation binding sites in close proximity to the substrate binding domain.

The Na⁺/dicarboxylate cotransporter (NaDC-1)¹ is situated in the apical membrane of renal proximal tubule cells where it reabsorbs tricarboxylic acid cycle intermediates, such as succinate and citrate, from the tubular filtrate (1). The uptake of citrate is particularly interesting because citrate provides a significant amount of substrate for renal proximal tubule cell oxidative metabolism (2) and is also necessary in the urine for prevention of calcium stone formation (3). NaDC-1 couples three sodium ions with the transport of each substrate molecule, carried in its divalent anion form (3). Sodium appears to be an essential activator that binds first to the transporter and triggers a conformational change, resulting in an increased affinity for substrate (4). The current secondary structure model of NaDC-1 contains 11 transmembrane domains (TMDs) and an extracellular N-glycosylated carboxy terminus (5).

The rabbit (rbNaDC-1) and human (hNaDC-1) transporter amino acid sequences are 78% identical (6). rbNaDC-1 and hNaDC-1 expressed in *Xenopus* oocytes have similar apparent affinities for substrates succinate and glutarate, but there are some functional differences that distinguish the two transporters (7). For example, the *K_m* for citrate is approximately 8-fold greater in hNaDC-1 than in rbNaDC-1 (7). There are also differences in cation binding between the

rabbit and human transporters; rbNaDC-1 has a greater apparent affinity for sodium than hNaDC-1 (7). In addition, low concentrations of lithium inhibit rabbit NaDC-1 by competing with sodium at one of the cation binding sites (8), whereas the human transporter is relatively insensitive to inhibition by lithium (7).

In this study, chimeras of the human and rabbit Na⁺/dicarboxylate cotransporters were created to localize the regions of the proteins responsible for the observed differences in substrate and cation handling. We find that interactions between transmembrane domains 7, 10, and 11 contribute to the differences in apparent citrate affinities. The differences in cation binding between the two transporters are determined primarily by residues in TMDs 10 and 11. Finally, TMD 11 of NaDC-1 contains residues that influence or define a portion of the cation binding site that is sensitive to inhibition by lithium. We conclude that portions of at least one sodium binding site and the substrate binding site are located in TMD 7, 10, and 11 and their adjacent extramembranous loops.

EXPERIMENTAL PROCEDURES

Construction of Chimeric Transporter cDNAs. Chimeric transporters from rbNaDC-1 and hNaDC-1 cDNAs in pSPORT 1 plasmid (Life Technologies, Inc.) were constructed using a combination of restriction enzyme sites and polymerase chain reaction (PCR). All of the constructs contained the 5' and 3' untranslated regions from rbNaDC-1; therefore, variations in protein expression were most likely determined by the coding regions of the constructs. Chimera junctions were made in areas of maximal sequence identity in areas outside of the putative transmembrane domains, and no foreign amino acids were introduced. All chimeras were confirmed by sequencing.

[†] This study was supported by U.S. Public Health Service Grants DK46269 and DK02429 and Institutional NRSA Grant HL07249.

* To whom correspondence should be addressed: Department of Physiology and Biophysics, University of Texas Medical Branch, Galveston, TX 77555-0641. Telephone: (409) 772-3434. Fax: (409) 772-3381. E-mail: ampajor@utmb.edu.

¹ Abbreviations: rbNaDC-1, rabbit Na⁺/dicarboxylate cotransporter; hNaDC-1, human Na⁺/dicarboxylate cotransporter; TMD, transmembrane domain; PCR, polymerase chain reaction; PNGase F, peptidyl N-glycanase F.

The amino acid sequence numbering is according to the rbNaDC-1 cDNA sequence (9). Junctions between TMDs 4 and 5 and between TMDs 10 and 11 were made at available native restriction sites, at nucleotides 525 (*SacI*) and 1616 (*SrfI*), respectively. Junctions between TMDs 7 and 8 and between TMDs 9 and 10 were created by engineering *NruI* restriction sites using the method of Kunkel (10) at nucleotides 1041 and 1467, respectively.

Junctions between TMDs 6 and 7 and between TMDs 8 and 9 were created using overlap extension PCR (11). The M13 forward primer was used together with the primers 5'-GTGGCTGCAGATCCTCTTCCTG-3' (corresponding to nucleotides 850–871) and 5'-CCCAGGACTGACCCAG-GACC CAG-3' (corresponding to nucleotides 1171–1193) to amplify the downstream end of the rabbit and human transporter cDNAs. The complementary primers were also synthesized and combined with the M13 reverse primer to amplify the upstream end of the transporter cDNA. The human and rabbit PCR products were gel purified and then combined for amplification of the chimeras with the M13 forward and reverse primers. The chimeric PCR products were cloned into pSPORT1 at the *NotI* and *SalI* restriction sites.

In Vitro cRNA Transcription. The rabbit, human, and chimeric NaDC-1 cDNAs were linearized with *NotI* or *XbaI* for use as a template. cRNA was transcribed in vitro using the T7 mMessage mMachine (Ambion) and purified on Sephadex G-50 Quick Spin columns (Boehringer Mannheim). The cRNAs were suspended in water to a final concentration of 1 $\mu\text{g}/\mu\text{L}$.

Xenopus Oocytes. Female *Xenopus laevis* were obtained from Nasco or Xenopus I. Stage V and VI oocytes were dissected and treated with collagenase as described previously (9). Oocytes were injected with 50 nL of cRNA on the following day. The oocytes were cultured at 18 °C in Barth's medium supplemented with 5% heat-inactivated horse serum, 2.5 mM pyruvate, and 50 mg/mL gentamicin. Culture dishes and medium were changed daily.

Immunodetection of Cell Surface-Expressed Transporters. Cell surface biotinylation and Western blotting were used to confirm protein expression and the correct masses of parental and chimeric transporters, as described previously (12). The oocytes were labeled with the membrane impermeant biotin reagent, Sulfo-NHS-LC-Biotin (Pierce), and the biotinylated proteins were precipitated using ImmunoPure Immobilized Streptavidin beads (Pierce). Because the parental transporters contain different numbers of N-glycosylation sites (rbNaDC-1 contains one N-glycosylation site and hNaDC-1 contains two sites), the biotinylated protein samples were deglycosylated using PNGase-F before separation of the proteins on tricine SDS-PAGE, as described previously (12). The proteins were blotted onto nitrocellulose membranes and probed with an anti-NaDC-1 antibody (12) applied at a dilution of 1:5000 for 2 h followed by incubation with horseradish peroxidase-linked anti-rabbit Ig (Amersham) at a dilution of 1:5000 for 1 h. Antibody binding to NaDC-1 was detected with the Supersignal CL-HRP substrate system (Pierce).

Transport Experiments. Uptake of [^{14}C]succinate [DuPont-New England Nuclear (NEN)] and [^{14}C]citrate (Moravsek Biochemicals and NEN) was assessed in groups of five oocytes between 4 and 6 days after cRNA injection. After

the samples were rinsed with choline buffer [100 mM choline chloride, 2 mM KCl, 1 mM MgCl_2 , 1 mM CaCl_2 , and 10 mM HEPES-Tris (pH 7.5)], transport was initiated with the appropriate substrate in sodium transport buffer (same as above but with 100 mM NaCl substituted for choline chloride). Transport was terminated with the addition of ice-cold choline buffer, followed by removal of extracellular radioactivity with three additional washes with cold choline buffer. Each oocyte was then transferred to a separate scintillation vial and dissolved in 0.25 mL of 10% SDS. Scintillation cocktail was added, and radioactivity was counted.









The specific conditions for each type of experiment are described as follows. To determine the ratios of citrate to succinate uptake, the rate of transport of 1 mM substrate was measured for 15 min. For lithium inhibition experiments, the rate of uptake of 100 μM succinate was measured for 15 min in transport buffers containing 97.5 mM NaCl and 2.5 mM choline chloride (control) or LiCl. For kinetic measurements, a master mix containing [^{14}C]citrate in sodium buffer was diluted to seven concentrations of citrate, between 100 μM and 7 mM, with equal specific activity at each concentration. In preliminary experiments with rbNaDC-1 and hNaDC-1, the rates of uptake of 1 and 5 mM citrate were linear to at least 10 min (results not shown). Therefore, 5 min uptakes were used for kinetic experiments with all samples except for chimera R11, which was measured for 30 min due to low activity. In sodium activation experiments, the sodium concentrations were varied between 0 and 150 mM by replacing with choline chloride. Kinetic constants were calculated by nonlinear regression with the Michaelis–Menten and Hill equations, using SigmaPlot 3.0 software (Jandel Scientific). Statistical analysis with a Student's *t* test was performed using SigmaStat (Jandel Scientific).

RESULTS

The C-Terminal Half of NaDC-1 Influences the Substrate Affinity. The first group of chimeric transporters between rbNaDC-1 and hNaDC-1 was constructed by combining up to eight transmembrane domains from the amino terminus of one parental transporter with the remaining carboxy terminus from the other parental transporter (Table 1). The chimera nomenclature consists of the letters H (human) and R (rabbit) followed by the number of transmembrane domains contributed by the parental transporter at the amino terminus. Chimeric transporters were expressed in *Xenopus* oocytes, and the transport activity was measured. The apparent K_m for citrate was determined in chimeras with high levels of expression. Because rbNaDC-1 and hNaDC-1 have similar K_m values for succinate (7), the ratio of uptake of 1 mM citrate to 1 mM succinate was also measured to allow some indication of relative citrate affinity in poorly expressed chimeras.







The rabbit transporter, rbNaDC-1, had a mean K_m for citrate of 0.9 mM (7) and a citrate:succinate transport ratio of 95%, whereas hNaDC-1 had a mean K_m for citrate of 7.2 mM (7) and a citrate:succinate uptake ratio of 26% (Table 1). Chimeras containing the first four or six transmembrane domains from hNaDC-1 and the rabbit C-terminus, HR-4 and HR-6, had citrate K_m values identical to that of the rabbit transporter, indicating that the C-terminal half of NaDC-1

Table 1: Citrate Transport in Parental and Chimeric NaDC-1 Transporters^a

Chimera	Citrate kinetics			Transport ratio ^b
	K _m (mM)	V _{max} (pmol/oocyte-hr)	N	
 Rabbit (R)	0.9 ± 0.1 ^c	11.5 ± 1.7 ^c	10 ^c	95 ± 4 (19)
 Human (H)	7.2 ± 0.5 ^c	20.0 ± 2.5 ^c	6 ^c	26 ± 1 (19)
 HR-4	0.9 ± 0.1	10.5 ± 0.9	3	131 ± 7 ^d (4)
 RH-4	N.D.	N.D.	-	37 ± 5 ^d (5)
 HR-6	0.8 ± 0.2	9.3 ± 1.1	4	92 ± 9 (5)
 RH-6	N.D.	N.D.	-	N.D.
 HR-8	2.4 ± 0.5 ^d	5.2 ± 1.6	3	75 ± 9 ^d (6)
 RH-8	N.D.	N.D.	-	27 ± 5 (3)

^a The black boxes in the chimera figures represent TMDs from rbNaDC-1; white boxes represent hNaDC-1. Values are means ± the standard error of the mean (SEM). The number of experiments, *N*, is shown in a column for citrate kinetics or in parentheses for transport ratios. ND indicates no data due to the low activity of chimeras. ^b Percent uptake of 1 mM citrate relative to the uptake of 1 mM succinate. ^c Value taken from ref 7. ^d Different from those of parental rbNaDC-1 and hNaDC-1 (*P* < 0.01).

Table 2: Citrate Transport by Chimeras Containing Substitutions of C-Terminal TMDs^a

Chimera	Citrate kinetics			Transport ratio ^b
	K _m (mM)	V _{max} (pmol/oocyte-hr)	N	
 HR-6	0.8 ± 0.2	9.3 ± 1.1	4	92 ± 9 (5)
 C-H7	2.8 ± 0.6 ^c	12.0 ± 4.0	6	53 ± 5 ^c (5)
 C-H8	0.7 ± 0.3	0.7 ± 0.4	3	108 ± 7 (6)
 C-H9	1.0 ± 0.5	1.8 ± 0.7	4	98 ± 8 (3)
 C-H10	2.5 ± 0.6 ^c	2.2 ± 0.6	3	50 ± 5 ^c (3)
 C-H11	3.0 ± 0.6 ^c	19.4 ± 3.9	3	64 ± 2 ^c (5)

^a The chimeras in this series are based on chimera HR-6 and contain substitutions in the carboxy-terminal portion of the transporter. The black boxes in the chimera figures represent TMDs from rbNaDC-1; white boxes represent hNaDC-1. The data for HR-6 are repeated from Table 1 for purposes of comparison. Values are means ± SEM. The sample size, *N*, is shown in a column for citrate kinetic data and in parentheses for transport ratios. ^b Percent uptake of 1 mM citrate relative to the uptake of 1 mM succinate. ^c Different from those of NaDC-1 and hNaDC-1 (*P* < 0.01).

three TMDs from rbNaDC-1, exhibited an intermediate phenotype with an apparent *K_m* for citrate of 2.4 mM and a citrate:succinate uptake ratio of 75% (Table 1). These data suggest that multiple determinants of citrate affinity exist and that they have been separated in HR-8.

Chimeras Containing Substitutions in the C-Terminus. A series of five chimeras (Table 2) was constructed to delineate the domains in the C-terminus that affect citrate affinity. Each of these chimeras contains TMDs 1–6 from hNaDC-1, which have no effect on the differences in citrate *K_m* but allow high levels of expression in oocytes. The last five TMDs from rbNaDC-1 were replaced with single TMDs from hNaDC-1 (Table 2). The chimeras in this group are designated by the letters C, for the carboxy-terminal half, and H, for hNaDC-1 substitution, followed by the substituted transmembrane domain number. As shown in Figure 1, all were expressed on the plasma membrane, although there were some differences in abundance. Chimeras C-H8 and C-H9, containing substitutions of TMD8 or TMD9, showed no change in the *K_m* for citrate compared with that of the parental HR-6, indicating that transmembrane domains 8 and 9 are not important for the differences in citrate affinity. However, chimeras with substitutions of transmembrane domain 7, 10, or 11 had intermediate citrate *K_m* values (Table 2). Therefore, each of these domains contributes to the measurable differences in citrate affinity between the rabbit and human NaDC-1.

Transmembrane Domains 7, 10, and 11 Determine the Differences in Apparent Citrate Affinities. In the third series of chimeras, TMDs 7, 10, and 11 from rbNaDC-1 were substituted, individually and together, into hNaDC-1 to assess their relative importance in the determination of apparent affinities. This series of chimeras is named "R" followed by the transmembrane domain number that was contributed by the rabbit transporter. Each chimera containing only one domain from the rabbit transporter had an apparent *K_m* for citrate that was intermediate between those of the two

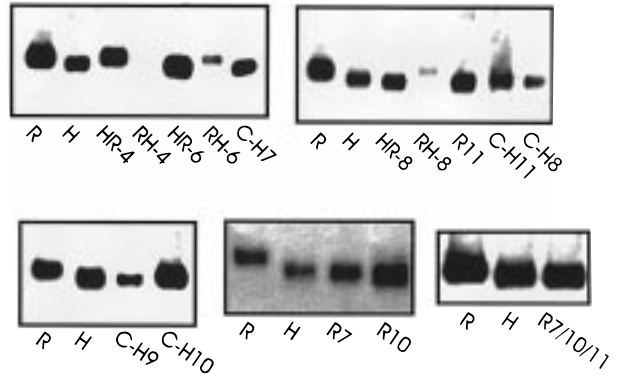






FIGURE 1: Western blots of cell surface-biotinylated proteins in oocytes expressing parental and chimeric NaDC-1 transporters. *Xenopus* oocytes were labeled using a membrane impermeant derivative of biotin, Sulfo-NHS-LC-Biotin (Pierce), as described in Experimental Procedures. Because rbNaDC-1 and hNaDC-1 have different numbers of N-glycosylation sites, all of the samples were deglycosylated using PNGase F. In these blots, deglycosylated rbNaDC-1 migrates at approximately 60.5 kDa and hNaDC-1 at approximately 59 kDa. Sample RH-4, although not visible in this exposure, was visible after exposing the film for a longer period of time (not shown).

influences substrate affinity. These chimeras were also well expressed at the plasma membrane (Figure 1). In contrast, chimeras RH-4, RH-6, and RH-8, containing the rabbit N-terminus, exhibited low levels of protein expression as measured by Western immunoblot analysis (Figure 1) and low transport activity. However, the ratio of citrate to succinate uptake measured in these chimeras was similar to the ratio seen in hNaDC-1 (Table 1), again suggesting that the determinants of differences in citrate affinity are present in the C-terminal half of the protein. Chimera HR-8, consisting of the first eight TMDs from hNaDC-1 and last

Table 3: Involvement of TMDs 7, 10, and 11 in Determining Relative Citrate Affinities^a


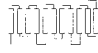





Chimera	Citrate kinetics			Transport ratio ^b
	K _m (mM)	V _{max} (pmol/oocyte-hr)	N	
 R7	4.2 ± 0.9 ^c	13.9 ± 3.9	5	51 ± 5 ^c (4)
 R10	3.7 ± 0.9 ^c	14.7 ± 2.8	5	49 ± 7 ^c (3)
 R11	4.5 ± 0.9 ^c	1.5 ± 0.6	3	29 ± 4 (5)
 R7/10/11	1.2 ± 0.3	5.1 ± 0.5	4	79 ± 4 (4)

^a TMDs 7, 10, and 11 from rbNaDC-1 were substituted into hNaDC-1. White boxes represent putative TMDs from hNaDC-1; black boxes represent TMDs from rbNaDC-1. Values are means ± SEM. *N* represents the sample size and is shown in the column for citrate kinetic data and in parentheses for transport ratio data. ^b Percent uptake of 1 mM citrate relative to the uptake of 1 mM succinate. ^c Different from those of rbNaDC-1 and hNaDC-1 (*P* < 0.05).

parental transporters, confirming that TMDs 7, 10, and 11 each contribute to citrate affinity (Table 3). The chimera R7/10/11 contains TMDs 7, 10, and 11 from rbNaDC-1 in an otherwise hNaDC-1 background. As indicated in Table 3, the measured *K_m* for citrate in R7/10/11 was 1.4 mM, very similar to the citrate *K_m* of the parental rbNaDC-1 and HR-6 transporters. Therefore, R7/10/11 contains the amino acids that are important in determining the observed differences in citrate affinity between rbNaDC-1 and hNaDC-1.

Differences in Sodium Affinity Are Also Determined by the C-Terminal Half of NaDC-1. In addition to differences in citrate affinity, rbNaDC-1 has a greater apparent sodium affinity than hNaDC-1 (7). In an ordered binding model of transport, the binding of sodium changes the transporter conformation such that it has a higher affinity for substrate. Therefore, it is possible that the differences in citrate affinity between rbNaDC-1 and hNaDC-1 are a consequence of their differences in sodium affinity. To test this hypothesis, the extent of sodium activation of succinate transport was measured for some of the chimeras (Table 4). In the previous study, a *K_{Na}* of 40 mM was measured for rbNaDC-1, but the *K_{Na}* of 78 mM for hNaDC-1 was an estimate because the maximum sodium concentration of 100 mM that was used did not saturate transport (7). In this study, the highest sodium concentration was increased to 150 mM, and under these conditions, the estimated apparent *K_{Na}* for hNaDC-1 was 141 mM while the apparent *K_{Na}* for rabbit rbNaDC-1 was unchanged at 44 mM (Table 4). As seen in previous studies, the apparent Hill coefficient for both transporters was between 1.4 and 2.5, consistent with the coupling stoichiometry of three Na⁺ ions per succinate (13, 14). Because the apparent *K_{Na}* of hNaDC-1 is close to the highest concentration of sodium that was used, the kinetic values for hNaDC-1 should be considered estimates. The sodium binding characteristics of the HR-6, R7/10/11, R10, and R11 chimeras were very similar to those of the rabbit transporter (Table 4). The R11 chimera had a slightly lower sodium affinity than rbNaDC-1 (apparent *K_{Na}* of 59 mM). In contrast, the apparent *K_{Na}* in R7 was similar to that of the human form (Table 4), suggesting that TMD 7 does not influence sodium affinity but that TMDs 10 and 11 each contribute to the differences in sodium affinity. Therefore, the differences in

Table 4: Involvement of TMDs 7, 10, and 11 in Determining Relative Sodium Affinities^a

Chimera	Sodium activation kinetics		
	<i>K_{Na}</i> (mM)	Hill coefficient, <i>n</i>	N
 Rabbit (R)	44 ± 5	1.4 ± 0.2	4
 Human (H)	141 ± 43	2.5 ± 0.4	3
 HR-6	34 ± 4	1.8 ± 0.2	4
 R7/10/11	46 ± 9	1.8 ± 0.3	3
 R7	110 ± 27	2.5 ± 0.5	3
 R10	51 ± 10	2.3 ± 0.4	3
 R11	60 ± 12	2.2 ± 0.3	3

^a Sodium activation of succinate transport experiments were conducted as described in Experimental Procedures. In the chimera figures, white boxes represent TMDs from hNaDC-1; black boxes represent those from rbNaDC-1. Values are means ± SEM. *N* is the sample size. The Hill coefficient is indicated as *n*.

apparent citrate affinity in rbNaDC-1 and hNaDC-1 are not solely a consequence of their differences in sodium affinity.

Inhibition of Chimera Transport Activity by Lithium. Rabbit rbNaDC-1 is inhibited by lithium with an IC₅₀ of about 2.5 mM, but hNaDC-1 is relatively insensitive to lithium (7). Lithium binds with high affinity to one of the sodium binding sites in NaDC-1 (8, 14). Therefore, localization of the domain that determines lithium sensitivity should identify a portion of one of the cation binding sites in NaDC-1. As seen previously (7), the transport activity of succinate by rbNaDC-1 was reduced to 46% of the control activity by 2.5 mM lithium, while the succinate transport of hNaDC-1 was unaffected (Figure 2). The HR-6 and R7/10/11 chimeric transporters were inhibited to 48 and 55% of control activity, respectively, suggesting that the C-terminal half of the transporter contains the lithium sensitive cation binding site. Substitution of individual TMDs showed that the lithium sensitivity was not associated with TMD 7 or 10. However, the R11 chimera was inhibited to 52% of control activity in the presence of lithium, similar to the parental rbNaDC-1 (Figure 2). Therefore, the determinants for lithium inhibition, which could represent part of a cation binding site, are located in TMD 11.

DISCUSSION

The analysis of chimeric transporters has allowed the localization of protein domains that are responsible for functional differences between the rabbit and human Na⁺/dicarboxylate cotransporters. We have found that transmembrane domains 7, 10, and 11 with their adjacent extracellular and intracellular segments are responsible for the functional differences between rbNaDC-1 and hNaDC-1, including apparent citrate affinity, sodium affinity, and lithium sensitivity. Each of the three domains contributes to differences in citrate affinity, and all three must interact to account for all of the measured differences between rbNaDC-1 and hNaDC-1. However, only two of the domains, TMD 10 and 11, are important in determining the differences in apparent

sodium affinity, and TMD 11 is solely responsible for the sensitivity to lithium. Therefore, the results suggest that at least one of the cation binding sites is located close to the substrate binding site in the carboxy terminus of the protein.

One notable difference in the transport properties between rbNaDC-1 and hNaDC-1 is in the apparent affinity for citrate (7). The K_m for citrate in rbNaDC-1 is approximately 0.9 mM, whereas the K_m for citrate in hNaDC-1 is approximately 7 mM (7). Although the differences in K_m are interpreted as differences in binding affinity, it should be noted that the K_m values measured in these studies could also be influenced by rate constants for steps after binding, such as translocation and dissociation. However, the results of these studies suggest that the determinants for the differences in apparent citrate affinity are located in the carboxy-terminal half of rbNaDC-1, specifically in putative transmembrane domains 7, 10, and 11. Interestingly, substitutions of individual transmembrane domains are not sufficient to confer the change in citrate K_m , which suggests that interactions between the three domains are necessary.

The localization of the determinants of species differences in substrate affinity in NaDC-1 to the carboxy terminus further defines the role of this region of the protein. Our previous study showed that the substrate recognition domain of rbNaDC-1 is also found in the carboxy terminus. A chimera consisting of the first four transmembrane domains from rbNaDC-1 and the last seven transmembrane domains from the Na⁺/sulfate transporter, NaSi-1, retained the substrate binding characteristics of NaDC-1 (15). There are also examples of other sodium-coupled transporters with substrate binding sites in the carboxy terminus, including Na⁺/glucose cotransporter SGLT1 (16, 17), Na⁺/nucleoside cotransporters SPNT and rCNT1 (18), and Na⁺/glutamate cotransporters EAAT1 and EAAT2 (19). However, there are sodium-coupled transporters, such as the dopamine and norepinephrine transporters, in which both the N- and C-termini appear to determine substrate affinity (20). It should be emphasized that our chimera studies address only differences in apparent substrate affinity between rbNaDC-1 and hNaDC-1; the N-terminus could play a critical, but identical role, in binding substrates in the two transporters.

In the current model of NaDC-1 function, sodium is an essential activator that binds to the transporter and causes an increase in the transporter's affinity for substrate. Studies with rabbit renal brush border membrane vesicles showed that the K_m for succinate increased as sodium concentrations were decreased (4). Because the apparent sodium affinity in hNaDC-1 is lower than in rbNaDC-1 (K_{Na} values of 141 and 44 mM, respectively) and the sodium concentration used for oocyte experiments is 100 mM, the levels of uptake in hNaDC-1 are measured at subsaturating sodium concentrations. Therefore, it is possible that the differences in apparent citrate affinity between rbNaDC-1 and hNaDC-1 are a consequence of the differences in their sodium affinity. Although chimera R7/10/11 had sodium and citrate K_m values that were similar to those of rbNaDC-1, the results with chimeras containing single transmembrane domain substitutions showed that the sodium and citrate affinities could be separated. For example, chimera R7, which contained transmembrane domain 7 from rbNaDC-1 substituted into hNaDC-1, exhibited intermediate citrate binding properties but the cation binding properties of hNaDC-1. Chimera R10

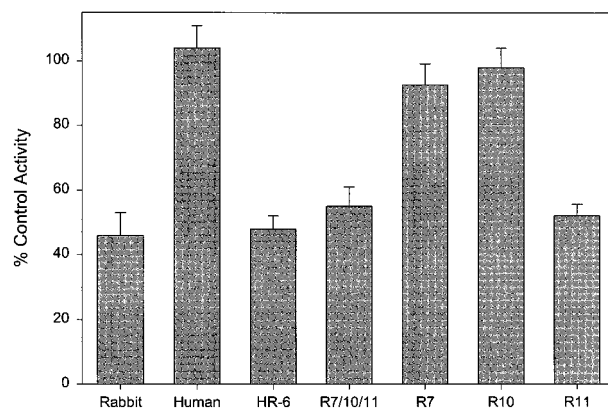


FIGURE 2: Lithium inhibition of succinate transport in parental and chimeric transporters expressed in *Xenopus* oocytes. The level of transport of 100 μ M succinate was measured for 15 min in the presence or absence (control) of 2.5 mM lithium. Bars represent uptake means \pm the standard error of the mean ($n = 3-6$) in the presence of lithium expressed as a percentage of control activity.

exhibited the sodium binding properties of rbNaDC-1, lithium binding properties of hNaDC-1, and intermediate citrate affinity. Therefore, the differences in citrate binding in rbNaDC-1 and hNaDC-1 are likely to be determined by sequence differences in the proteins and are not solely a consequence of sodium affinity.

Our results indicate that transmembrane domain 11 contains or influences one of the three sodium binding sites in rbNaDC-1. Low concentrations of lithium inhibit rbNaDC-1, but not hNaDC-1, by competing with sodium at one high-affinity cation binding site. Lithium binding does not appear to produce the optimal conformation for transport, as the K_m for succinate measured in lithium is 30 mM (8, 14). Chimera R11, containing transmembrane domain 11 from rbNaDC-1 and TMDs 1-10 from hNaDC-1, had the characteristic lithium sensitivity of rbNaDC-1. Therefore, TMD 11 is likely to contain all or part of a sodium binding site that is also the site for high-affinity lithium binding in NaDC-1. Alternatively, TMD 11 could be important in the cation-induced conformational change of NaDC-1. In either case, this finding establishes a new role for the last transmembrane domain in NaDC-1.

There is little information about the location of cation binding sites in Na⁺-coupled transporters. The *Escherichia coli* melibiose transporter, *MelB*, transports sugars by coupling with Na⁺, Li⁺, or H⁺ (21). Chimera studies with *MelB* and its homologues suggest that residues from both the amino and carboxy termini are necessary for binding sodium (22). SGLT1 also appears to require the amino terminus for cation binding. A construct of SGLT1 containing only the carboxy-terminal half of the protein functions as a cation-independent facilitative carrier of glucose, suggesting that at least part of the sodium binding domains are in the amino-terminal half of the protein (17). NaDC-1 could have cation binding sites formed by both the amino and carboxy termini, but the residues that are critical for the differences in sodium affinity are located in TMDs 10 and 11.

The characterization of chimeric transporters has identified three regions of the protein likely to be responsible for many of the functional differences between rabbit and human NaDC-1. Chimera R7/10/11, which contains all of the residues necessary for conferring the differences in citrate

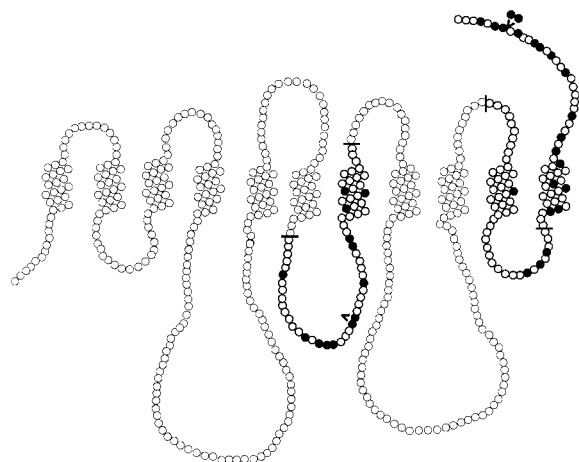


FIGURE 3: Secondary structure model of rabbit rbNaDC-1 showing the regions important in determining differences in citrate and sodium affinity. The junctions used in constructing chimera R7/10/11 are denoted with lines. The filled circles represent amino acids that differ between rabbit and human NaDC-1 in the domains determined to affect citrate and sodium affinity. The \rightarrow indicates the location of amino acid insertions or deletions compared with hNaDC-1.

K_m values, contains only 35 amino acids that differ between the two transporters (Figure 3). Chimeras R10 and R11, containing the residues that determine differences in K_{Na} values and lithium sensitivity, contain 22 amino acids that are different in rbNaDC-1 and hNaDC-1. The residues most likely to be involved in cation or substrate binding are polar and acidic residues, which further narrows down the possible candidates. Future studies using site-directed mutagenesis will aim to identify the critical amino acids in chimera R7/10/11 that determine the functional differences in rbNaDC-1 and hNaDC-1. In conclusion, these studies show that the substrate and at least one of the cation binding sites are found in the carboxy-terminal portion of the protein. In particular, a portion of the high-affinity cation binding site that is sensitive to inhibition by lithium is likely to be located in transmembrane domain 11.

ACKNOWLEDGMENT

We thank Nina Sun and Marci Price for assistance with oocyte experiments, Suzanne Watson for construction of

chimeras HR-4 and RH-4, and Dr. Doug Griffith for many helpful discussions.

REFERENCES

1. Pajor, A. M. (1999) *Annu. Rev. Physiol.* 61, 663–682.
2. Simpson, D. P. (1983) *Am. J. Physiol.* 244, F223–F234.
3. Hamm, L. L. (1990) *Kidney Int.* 38, 728–735.
4. Wright, S. H., Hirayama, B., Kaunitz, J. D., Kippen, I., and Wright, E. M. (1983) *J. Biol. Chem.* 258, 5456–5462.
5. Pajor, A. M., and Sun, N. (1996) *Am. J. Physiol.* 271, C1808–C1816.
6. Pajor, A. M. (1996) *Am. J. Physiol.* 270, F642–F648.
7. Pajor, A. M., and Sun, N. (1996) *Am. J. Physiol.* 271, F1093–F1099.
8. Wright, E. M., Wright, S. H., Hirayama, B. A., and Kippen, I. (1982) *Proc. Natl. Acad. Sci. U.S.A.* 79, 7514–7517.
9. Pajor, A. M. (1995) *J. Biol. Chem.* 270, 5779–5785.
10. Kunkel, T. A. (1985) *Proc. Natl. Acad. Sci. U.S.A.* 82, 488–492.
11. Ho, S. N., Hunt, H. D., Horton, R. M., Pullen, J. K., and Pease, L. R. (1998) *Gene* 77, 1–59.
12. Pajor, A. M., Sun, N., and Valmonte, H. G. (1998) *Biochem. J.* 331, 257–264.
13. Hirayama, B., and Wright, E. M. (1986) *Pfluegers Arch.* 407 (Suppl. 2), S174–S179.
14. Pajor, A. M., Hirayama, B. A., and Loo, D. D. F. (1998) *J. Biol. Chem.* 273, 18923–18929.
15. Pajor, A. M., Sun, N., Bai, L., Markovich, D., and Sule, P. (1998) *Biochim. Biophys. Acta* 1370, 98–106.
16. Panayotova-Heiermann, M., Loo, D. D. F., Kong, C.-T., Lever, J. E., and Wright, E. M. (1996) *J. Biol. Chem.* 271, 10029–10034.
17. Panayotova-Heiermann, M., Eskandari, S., Turk, E., Zampighi, G. A., and Wright, E. M. (1997) *J. Biol. Chem.* 272, 20324–20327.
18. Wang, J., and Giacomini, K. M. (1997) *J. Biol. Chem.* 272, 28845–28848.
19. Mitrovic, A. D., Amara, S. G., Johnston, G. A. R., and Vandenberg, R. J. (1998) *J. Biol. Chem.* 273, 14698–14706.
20. Buck, K. J., and Amara, S. G. (1994) *Proc. Natl. Acad. Sci. U.S.A.* 91, 12584–12588.
21. Tsuchiya, T., and Wilson, T. H. (1978) *Membr. Biochem.* 2, 63–79.
22. Hama, H., and Wilson, T. H. (1993) *J. Biol. Chem.* 268, 10060–10065.

BI9827722